

3-2012

Photochemistry Of Monochloro Complexes Of Copper(ii) In Methanol Probed By Ultrafast Transient Absorption Spectroscopy

Andrey S. Mereshchenko

Suman K. Pal


Kanykey E. Karabaeva

Patrick Z. El-Khoury

Alexander N. Tarnovsky

Bowling Green State University, atarnov@bgsu.edu

Follow this and additional works at: https://scholarworks.bgsu.edu/chem_pub

 Part of the [Chemistry Commons](#)

Repository Citation

Mereshchenko, Andrey S.; Pal, Suman K.; Karabaeva, Kanykey E.; El-Khoury, Patrick Z.; and Tarnovsky, Alexander N., "Photochemistry Of Monochloro Complexes Of Copper(ii) In Methanol Probed By Ultrafast Transient Absorption Spectroscopy" (2012). *Chemistry Faculty Publications*. 117.
https://scholarworks.bgsu.edu/chem_pub/117

This Article is brought to you for free and open access by the Chemistry at ScholarWorks@BGSU. It has been accepted for inclusion in Chemistry Faculty Publications by an authorized administrator of ScholarWorks@BGSU.

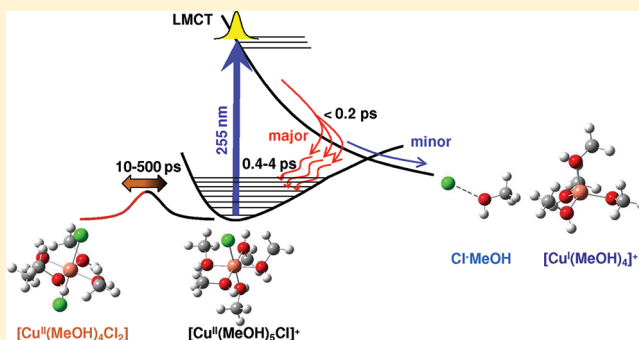
Photochemistry of Monochloro Complexes of Copper(II) in Methanol Probed by Ultrafast Transient Absorption Spectroscopy

Andrey S. Mereshchenko, Suman K. Pal,[†] Kanykey E. Karabaeva, Patrick Z. El-Khoury,[‡] and Alexander N. Tarnovsky*

Department of Chemistry and Center for Photochemical Sciences, Bowling Green State University, Bowling Green, Ohio 43403, United States

S Supporting Information

ABSTRACT: Ultrafast transient absorption spectra in the deep to near UV range (212–384 nm) were measured for the $[\text{Cu}^{\text{II}}(\text{MeOH})_5\text{Cl}]^+$ complexes in methanol following 255-nm excitation of the complex into the ligand-to-metal charge-transfer excited state. The electronically excited complex undergoes sub-200 fs radiationless decay, predominantly via back electron transfer, to the hot electronic ground state followed by fast vibrational relaxation on a 0.4–4 ps time scale. A minor photochemical channel is Cu–Cl bond dissociation, leading to the reduction of copper(II) to copper(I) and the formation of $\text{MeOH}\cdot\text{Cl}$ charge-transfer complexes. The depletion of ground-state $[\text{Cu}^{\text{II}}(\text{MeOH})_5\text{Cl}]^+$ perturbs the equilibrium between several forms of copper(II) complexes present in solution. Complete re-equilibration between $[\text{Cu}^{\text{II}}(\text{MeOH})_5\text{Cl}]^+$ and $[\text{Cu}^{\text{II}}(\text{MeOH})_4\text{Cl}_2]$ is established on a 10–500 ps time scale, slower than methanol diffusion, suggesting that the involved ligand exchange mechanism is dissociative.



INTRODUCTION

Copper plays a significant role in metabolism in the human body. Copper enzymes perform important functions such as the catalysis of biological reactions (for example, conversion of dopamine to noradrenaline^{1,2}), electron transfer, and protection of cells against free radicals.³ Copper metabolism infringement leads to arthritis,⁴ mental disorders,⁵ loss of fertility,⁶ and even to life-threatening diseases such as Menkes' syndrome^{7–9} and Wilson's disease.^{3,10,11}

Copper is a first row transition metal element, and its common cation, copper(II), has the d^9 configuration. For complexes of first row transition elements with inorganic ligands, an octahedral surrounding is most dominant (coordination number of six).¹² However, the Jahn–Teller effect¹² is very strong in the d^9 configuration, which leads to a geometrical distortion of the complex, and symmetry lowering from the O_h to D_{4h} or C_{4v} point groups. This is accompanied by an increase in bond lengths between the metal center and axial ligands.^{12–15} In solution, this effect is dynamic in nature, the distortion axis alternating rapidly, and all ligands sampling both axial and equatorial positions as a function of time.¹⁶ In extreme cases, if the bond length between the metal center and one or two axial ligands is much longer than the metal-equatorial ligand bond lengths, the geometries of these complexes may be viewed as square pyramid (coordination number of five) or square planar (coordination number of four), respectively. For example, a copper(II) cation exists as a distorted octahedral $[\text{Cu}^{\text{II}}(\text{MeOH})_6]^{2+}$ in methanol¹⁷ and as square planar

$[\text{Cu}^{\text{II}}(\text{MeCN})_4]^{2+}$ and $[\text{Cu}^{\text{II}}(\text{dmsO})_4]^{2+}$ complexes in acetonitrile and dimethyl sulfoxide solutions,¹⁸ respectively. In water, copper(II) ions are thought to exist as a mixture of penta- and hexa-coordinated complexes.^{14,15,19–21} The elongation of axial bonds weakens bond strengths and renders ligands in axial positions very labile. Indeed, ligand exchange rates of copper(II) complexes are one of the highest among coordination complexes of transition elements.^{13,16} Recent neutron diffraction and first-principle molecular dynamics studies of aqueous solution of copper(II) revealed the evolution with time constants 5 and 175 ps (corresponding to rates of 2×10^{11} and $5.7 \times 10^9 \text{ s}^{-1}$) which were attributed to the mean structural relaxation lifetime and the residence time of a water molecule in the first solvation shell.^{16,21} Early NMR studies were performed with a time resolution of several nanoseconds, and yielded $3.09 \times 10^7 \text{ s}^{-1}$ for the inverse lifetime of a methanol molecule in the first solvation shell.¹⁷

The focus of this work is the photochemistry of copper(II) halide complexes. Detailed studies of photoreactions of copper(II) salts began in the 60s, with growing interest in solvent effects and ligand tuning. In many studies, the photoreaction mechanism of CuX_2 ($X = \text{CH}_3\text{COO}^-$, Cl^- , Br^- , ClO_4^-) salts in solution

Special Issue: Femto10: The Madrid Conference on Femtochemistry

Received: September 5, 2011

Revised: October 22, 2011

Published: November 28, 2011

takes place via the radical dissociation process caused by ligand-to-metal charge transfer (LMCT) excitation. Photodissociation can be considered as either direct, $[\text{Cu}^{\text{II}}\text{Cl}_n]^{2-n} \xrightarrow{h\nu} [\text{Cu}^{\text{I}}\text{Cl}_{n-1}]^{2-n} + \text{Cl}^\bullet$, or proceeding via a long-lived charge-transfer excited state, $[\text{Cl}_{n-1}^- \text{Cu}^+ \text{Cl}^\bullet]^{2-n}$, as suggested by Kochi.²² It is well-known that copper perchlorate in methanol exists in the form of the solvated copper(II) cation, $[\text{Cu}^{\text{II}}(\text{MeOH})_6]^{2+}$. Silva and David²³ proposed that the first step following photoexcitation of solvated $[\text{Cu}(\text{MeOH})_6]^{2+}$ into its LMCT band using ultraviolet (UV) light in the 200–250 nm range is the dissociation of the parent complex into two products: the solvated complex of copper(I) ion ($[\text{Cu}(\text{MeOH})_5]^{+}$), and positively charged methanol CH_3OH^+ species which reacts further and ultimately leads to the formation of formaldehyde. The photoreaction of copper(II) chloride and bromide in methanol was also investigated by the same authors in greater details.²⁴ These systems reveal the same photoprocesses as the methanol solution of $\text{Cu}(\text{ClO}_4)_2$, but also exhibit different mechanisms for the formation of formaldehyde. In addition to the $[\text{Cu}^{\text{II}}(\text{MeOH})_6]^{2+}$ ion present in solution, copper(II) cations also form complexes with chloride and bromide anions, $[\text{Cu}(\text{MeOH})_{6-n}\text{X}_n]^{2-n}$ ($\text{X} = \text{Cl}^-, \text{Br}^-; n = 1-4$). These complexes also take part in the photochemical reactions. Upon UV irradiation, chloro and bromo complexes of copper(II) dissociate to copper(I) complexes and halogen radicals. The latter reacts with methanol to produce formaldehyde. According to David and Silva,²⁴ differently substituted $[\text{Cu}(\text{MeOH})_{6-n}\text{X}_n]^{2-n}$ ($\text{X} = \text{Cl}^-, \text{Br}^-; n = 1-4$) halide complexes afford copper(I) complexes in varying quantum yields upon UV irradiation. The yields are under 10% for the chloro-substituted copper(II) complexes, but increase significantly for the bromo complexes.²⁴ The photodissociation mechanism of chloro complexes proposed by David and Silva²⁴ was confirmed by Kaczmarek et al.²⁵ Glebov and coauthors²⁶ proposed that in the case of copper(II) acetate, the photoreaction mechanism involves the photoreduction of copper(II) to copper(I) through a long-lived CT excited state: $\text{Cu}(\text{CH}_3\text{COO})_2 \xrightarrow{h\nu} \text{CH}_3\text{COO}^- \text{Cu}^+ \text{OOCH}_3^\bullet \rightarrow \text{CH}_3\text{COOCu} + \text{OOCH}_3^\bullet$. Similarly, small photolysis quantum yields were reported, of about 0.8 and 0.25% in methanol and *iso*-propanol solutions, respectively.²⁶ This points to the presence of competing fast relaxation pathways, and further motivates the present work.

To sum up, in the aforementioned photochemical measurements, the authors mainly utilized steady-state methods such as colorimetry^{23,24} and steady state spectrophotometry^{25,26} to identify the products and measure their concentrations at relatively long times after photoirradiation. Although diffraction and NMR measurements allow for the structural characterization of some product species, the transient relaxation following photoexcitation remains largely unknown. For example, one of the conjectured intermediates is an ion-radical complex of copper (long-lived charge-transfer excited state), $[\text{Cl}_{n-1}^- \text{Cu}^+ \text{Cl}^\bullet]^{2-n}$.^{25,26} Small photolysis quantum yields reported strongly suggest the presence of competing photochemical mechanisms, which occur on ultrafast time scales and, therefore, require tools of ultrafast spectroscopy for “real-time” monitoring and characterization. In this work, we studied a monochloropentamethanol copper(II) complex, $[\text{Cu}(\text{MeOH})_5\text{Cl}]^+$, expected to exhibit a simple reaction mechanism that may be extended toward understanding more complex systems. The radiationless relaxation pathways of this complex in methanol solutions were investigated using femtosecond transient absorption spectroscopy with deep-near UV probing (212–384 nm). We report that the photochemical reaction path of this complex includes ultrafast efficient internal

conversion, which predominates over the previously reported photodissociation path.

EXPERIMENTAL SECTION

The ultrafast transient absorption setup used in this work has been previously described elsewhere.^{27,28} Briefly, a regeneratively amplified Ti:sapphire laser system (Hurricane, Spectra-Physics) generates a 1 kHz train of 90-fs (fwhm), 800-nm laser pulses with an energy of $0.92 \text{ mJ pulse}^{-1}$. The amplified output is 50:50 split into two beams. The first beam is delivered to a TOPAS-C “pump” optical parametric amplifier (Light Conversion Ltd.) to generate the second harmonic of the sum frequency of the fundamental and signal output beams (SHSFS), 255 nm pulses, used to excite the copper(II) complex. The second beam was further split 40:10 with the largest portion delivered to the TOPAS-C “probe” optical parametric amplifier to generate the analyzing beam as (i) the fourth harmonic of the signal output, FHS pulses tunable from 275 to 384 nm, (ii) sum-frequency of the FHS output and 10% portion of the amplified beam, pulses tunable from 210 to 265 nm, and (iii) sum-frequency of the fourth harmonic of the idler output and 10% portion of the amplified beam, pulses tunable from 267 to 300 nm. The analyzing beam was sent to the delay line, and further split into the reference and probe beams. The probe (passing through the sample) and reference beams are sent to the monochromator, and registered using two photodiodes. The transient absorption ΔA signals measured at single probe wavelengths from 212 to 384 nm and at time delays between -10 and $+1050$ ps were corrected for chirp and used to construct transient absorption spectra. The pump and probe beams are made to overlap at an angle of 8° at the sample position, and their diameters were measured to be 500 and $150 \mu\text{m}$, respectively. Using a Berek compensator in the path of the pump beam, its polarization is set at the magic angle (54.7°) with respect to that of the probe beam. The 312-nm ΔA signals were linearly proportional to excitation pulse energy in the $2.4-7 \mu\text{J}$ range, see the Supporting Information. Consequently, a pulse energy of $5.4 \mu\text{J}$ was selected for sample excitation. The sample was flown through a 0.2-mm flow cell. The width of the apparatus response function was determined using simultaneous absorption of two (pump and probe) photons in methanol.^{29,30} It manifests itself as a bell-like ΔA signal centered at zero time delay between the pump and probe pulses with a width (fwhm) increasing with an increase in probe photon energy, changing from 150 fs at 380 nm (near-UV or UVA) to 270 fs at 280 nm (low-energy wing of the deep-UV range or UVB) and 600 fs at 214 nm (high-energy wing of the deep-UV range or UVC). Steady-state spectra were measured using the Varian Cary 50 UV/vis spectrophotometer in a 0.2-mm quartz cell. Copper(II) perchlorate hexahydrate and lithium chloride were dissolved in methanol. The solution was then centrifuged to remove insoluble precipitate arising from crystal carbonates present in the solid sample of copper(II) perchlorate hexahydrate. To characterize the charge-transfer (CT) absorption band of a $\text{MeOH} \cdot \text{Cl}$ complex, solutions of chloroacetone (500 mM) in methanol were excited at 266 nm, and the transient absorption ΔA spectra were acquired in the 300–380 nm range at a 500-ps time delay (excitation energy, $5.4 \mu\text{J pulse}^{-1}$; 0.2-mm flow cell). All measurements were performed at the temperature of 22°C .

Copper(II) perchlorate hexahydrate (98%), lithium chloride (>99%), copper powder (>99%), acetyl acetone (99.5%), acetic acid acetonitrile (>99.5%), and methanol (>99.8%) were purchased

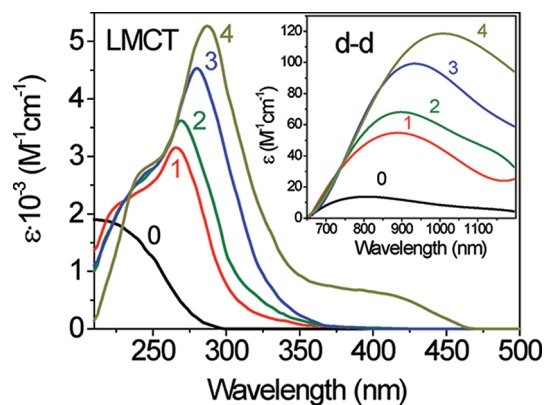


Figure 1. Steady-state absorption spectra of individual chloro complexes of copper(II) in methanol, $[\text{Cu}^{\text{II}}(\text{MeOH})_{6-n}\text{Cl}_n]^{2-n}$, where $n = 0-4$, taken from the literature.³²

from Sigma Aldrich and used without additional purification. Chloroacetone (95%) and ammonium acetate (HPLC grade) were purchased from Alfa Aesar and Fisher, respectively, and used without additional purification. Tetrakis(acetonitrile) copper(I) perchlorate was prepared by the reduction of copper(II) perchlorate by copper powder in acetonitrile, followed by drying under argon.³¹

RESULTS

Steady-State Measurements. In methanol solutions, copper(II) ions mostly exist as $[\text{Cu}^{\text{II}}(\text{MeOH})_6]^{2+}$.^{23,32} Additions of chloride ions leads to the formation of highly labile chloro complexes $[\text{Cu}^{\text{II}}(\text{MeOH})_{6-n}\text{Cl}_n]^{2-n}$ ($n = 1-4$), possessing different electronic absorption spectra^{32,33} (Figure 1). Their equilibrium concentrations are dictated by the initial concentrations of copper(II) and chloride ions. Relative concentrations of chloro complexes were estimated using the “Medusa” software, developed by the Royal Institute of Technology (KTH), Sweden.³⁴ For our calculations, we used the following overall stability constants: $\beta_1 = 2.8 \times 10^2$, $\beta_2 = 1.6 \times 10^4$, $\beta_3 = 2.3 \times 10^5$, and $\beta_4 = 4.5 \times 10^5$.³² The initial concentration of copper(II) was fixed at 50 mM and the concentration of chloride ions was varied between zero and 100 mM. The calculated fractional distribution of chloro complexes is shown in Figure 2. To maximize the relative concentration of the monochloropentamethanol copper(II) complex in the experiments, the initial concentration of chloride ions was set to 25 mM. Under these conditions, 96% of copper(II) is present as a mixture of unsubstituted ($[\text{Cu}^{\text{II}}(\text{MeOH})_6]^{2+}$, 58%), monochlorosubstituted ($[\text{Cu}^{\text{II}}(\text{MeOH})_5\text{Cl}]^+$, 38%) complexes, with a 4% contribution from $[\text{Cu}^{\text{II}}(\text{MeOH})_4\text{Cl}_2]$, Figure 2. Furthermore, the measured steady-state spectra of the 50 mM $\text{Cu}(\text{ClO}_4)_2/25$ mM LiCl solution in methanol can be fitted to a sum of the absorption spectra of these three copper complexes (Figure 2). In the fitting procedure, the known molecular extinction coefficients were held constant and the concentrations were varied to produce the best fit. The resulting fractional distribution of chloro complexes in the prepared solution is as follows: 44% of $[\text{Cu}^{\text{II}}(\text{MeOH})_6]^{2+}$, 49% of $[\text{Cu}^{\text{II}}(\text{MeOH})_5\text{Cl}]^+$, and 7% of $[\text{Cu}^{\text{II}}(\text{MeOH})_4\text{Cl}_2]$. The relative concentrations obtained from the fit and “Medusa” program agree reasonably well. The small difference in values arises from the “Medusa” program not taking into account the ionic strength of the solution. Using this output, the excitation wavelength in transient absorption experiments was set to 255 nm to preferentially excite the $[\text{Cu}^{\text{II}}(\text{MeOH})_5\text{Cl}]^+$ complex.

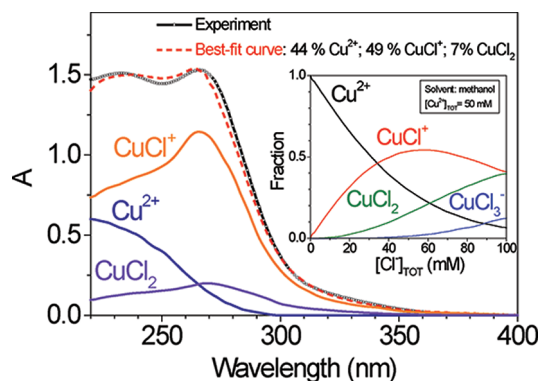


Figure 2. Steady-state absorption spectrum of a methanol solution containing $\text{Cu}(\text{ClO}_4)_2$ (50 mM) and LiCl (25 mM) measured in a 0.2-mm cell (line and symbols). The best-fit spectrum obtained using the known ϵ values of the individual copper(II) complexes as the parameters and their fractional concentrations as the variables is shown by a dashed line. The distribution of chloro complexes of copper(II) as function of concentration of chloride ions was also calculated by Medusa software (inset) using the following overall stability constants $\beta_1 = 2.8 \times 10^2$, $\beta_2 = 1.6 \times 10^4$, $\beta_3 = 2.3 \times 10^5$, and $\beta_4 = 4.5 \times 10^5$.³²

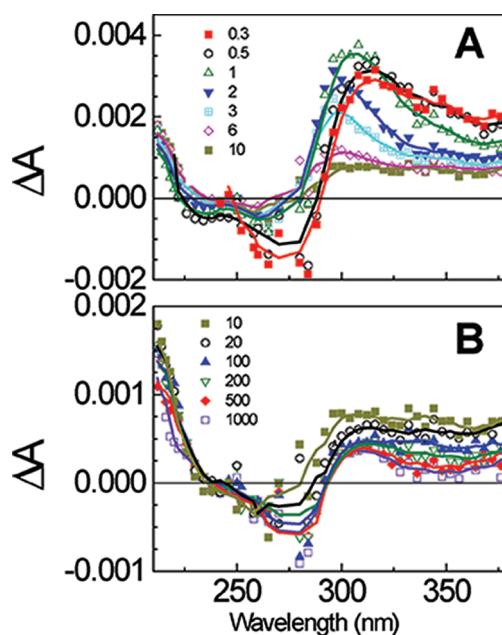


Figure 3. Transient absorption spectra of a 50 mM $\text{Cu}(\text{ClO}_4)_2/25$ mM LiCl methanol solution following 255-nm excitation with an energy of $5.4 \mu\text{J pulse}^{-1}$. Time delays given in the legends are expressed in picoseconds. Panels A and B show the short and long time delays, respectively.

To characterize the UV–vis spectrum of a thermally stable copper(I) solvated complex in methanol, tetrakis(acetonitrile) copper(I) perchlorate (3 mM) was dissolved in deoxygenated methanol. Because of vast excess of methanol, acetonitrile molecules in the first coordination sphere are replaced by methanol molecules. EXAFS studies showed that copper(I) cations in solution form tetrahedral $[\text{Cu}^{\text{I}}(\text{solvent})_4]^+$ complexes with solvents such as acetonitrile, dimethylsulfoxide, pyridine, and tetrahydrothiophene.¹⁸ Similarly, copper(I) solvated complexes are expected to adopt the tetrahedral $[\text{Cu}^{\text{I}}(\text{MeOH})_4]^+$

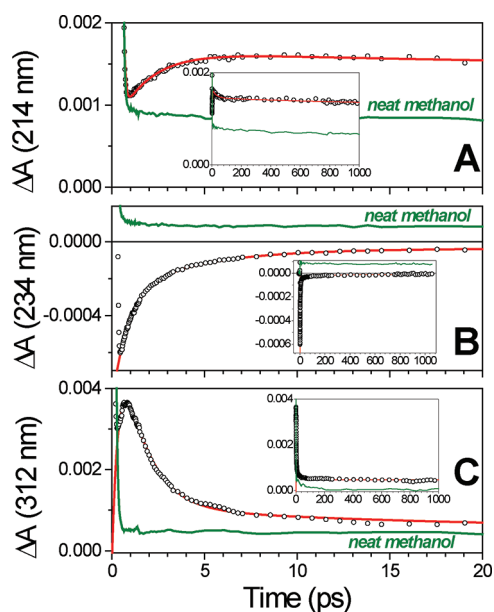


Figure 4. Short-time transient absorption kinetic traces (symbols) of a 50 mM $\text{Cu}(\text{ClO}_4)_2/25$ mM LiCl methanol solution following 255-nm excitation ($5.4 \mu\text{J pulse}^{-1}$) measured at probe wavelengths of 214 nm (A), 234 nm (B), and 312 nm (C). Multiexponential fits (red lines) and short-time ΔA signals measured in neat methanol (green lines) are also shown. The insets display the same ΔA kinetic traces measured up to long time delays.

structure in methanol. The electronic spectrum of $[\text{Cu}^{\text{I}}(\text{MeOH})_4]^+$ consists of an intense band peaking at 211 nm ($\epsilon = 6780 \text{ M}^{-1} \text{ cm}^{-1}$) with two shoulders at about 240 and 290 nm (Figure 5).

Formaldehyde was detected in 50 mM $\text{Cu}(\text{ClO}_4)_2/25$ mM LiCl methanol solutions exposed to 255 nm light (by reaction with acetylacetone and ammonium acetate³⁵) but not in light-deprived copper(II) methanol solutions.

Ultrafast Transient Absorption Measurements. Ultrafast time-resolved transient absorption ΔA spectra following 255-nm excitation of 50 mM $\text{Cu}(\text{ClO}_4)_2/25$ mM LiCl methanol solution are shown in Figure 3. In comparison to the transient absorption of the sample solution, the ΔA signal from neat methanol measured upon identical excitation conditions becomes weak starting from a time delay, comparable to a half-width of the apparatus response function, all at the same single probe wavelength. Actual contribution of the former to the total ΔA signal should be further reduced by a factor of at least 2 because of the solute absorption, as estimated from the comparison of ΔA signals at zero time delay for neat methanol and sample solutions. A significant solvent contribution from 212 nm to 280 and 248 nm persists in the ΔA spectra measured at 0.2 and 0.3 ps, respectively. We conclude that the methanol contribution to ΔA spectra of the sample solution is minor at a time delay of 0.5 ps. At this time delay, broad transient absorption from 310 to 384 nm (already present at the shortest time delay of 0.2 ps), as well as negative ΔA signals between 225 and 290 nm due to the depletion of ground-state species are observed. In the 212–224 nm range, weak transient absorption is observed.

The description of the ΔA time evolution of the selected kinetics traces shown in Figure 4 was obtained by a fit to a sum of four exponential functions and an offset. At 214 nm, the best-fit time constants obtained were: $\tau_2 \approx 2.2 \pm 0.2$ ps (rise, major),

$\tau_3 \approx 26$ ps (decay, minor), and $\tau_4 \approx 5800$ ps (decay), whereas τ_1 could not be resolved because of the solvent contribution. The kinetic trace measured at 312 nm shows that the initial fast $\tau_1 = 0.4 \pm 0.1$ ps rise of the signal is followed by a decay of $\tau_2 = 1.1 \pm 0.3$ ps (both major), followed by longer decays with $\tau_3 \approx 13$ ps (minor) and $\tau_4 = 170 \pm 40$ ps (minor). Slower rise and decay times are observed at 234 nm ($\tau_1 = 0.69 \pm 0.07$ ps and $\tau_2 = 3.8 \pm 0.5$ ps, both major), whereas two other minor components 170 \pm 40 ps (similar to 312 nm) and 5800 ps (similar to 212 nm) were recorded.

A more complete picture of the dynamics is illustrated by the time evolution of the transient absorption spectra (Figure 3). Between 0.3 and 1 ps, broad transient absorption spectrally narrows to form a maximum at 306 nm (rise time constant, 400 fs, Figure 4C). Spectral narrowing is accompanied by a blue shift which cancels the ground-state bleach signal between 280 and 285 nm. Between 2 and 10 ps, the 306-nm feature decay (a time constant of 1.1 ps, Figure 4C) is accompanied by a partial recovery of the ground-state bleach. The remaining broad absorption in ~ 280 –384 nm range undergoes some decay and reshaping, manifested by the spectral shift of the $\Delta A = 0$ crossing point first to the blue (up to 6 ps) and then to the red. At the highest energy wing of the investigated spectrum, a rise of the ΔA signal is observed (time constant, 2.2 ps, Figure 4A). Following this rise, the ΔA signal in this range remains constant for tens of picoseconds before exhibiting a minor decay on a 200–1000 ps time scale. The exponential fit yields a 5.8 ns decay time constant for this process. Although the determination of this time constant is imprecise because we only trace a portion of the total evolution, it can be safely concluded that the process occurs on a time scale of about 10 ns. From 10 to 1000 ps, a gradual development of the negative ΔA signal occurs between 258 and 293 nm without any change in the negative signal amplitude from 237 to 258 nm. At the same time, the intensity of the broad absorption band in the UV range (295–380 nm) significantly decreases. The time constant for this evolution is about 150–220 ps, estimated based on the decay of the integrated transient absorption signal in the UVA part of the probe spectrum. This is consistent with the 170 ps component observed in the fits of the 234 and 312 nm kinetic traces.

To identify the presence of a $\text{Cl}\cdot$ atom fragment in the time-resolved spectra of $[\text{Cu}^{\text{II}}(\text{MeOH})_5\text{Cl}]^+$ in methanol, the absorption of the ensuing $\text{MeOH}\cdot\text{Cl}$ charge-transfer (CT) complex was identified. Here, methanol solutions of chloroacetone, a well-known precursor of chlorine atoms,^{36–38,43} was photolyzed using 100-fs, 266-nm laser pulses. On a sub-500 ps time scale, the photochemical reaction is found to involve long-lived species, tentatively attributed to low-lying triplet states of $\text{CH}_3\text{C}(\text{O})\text{CH}_2\text{Cl}$, similar to $\text{C}_6\text{H}_5\text{Br}$.⁴⁴ At 500 ps, the ΔA spectrum shows two absorption bands due to the photolysis products. A broad band centered at 320 nm is assigned to the absorption of the $\text{MeOH}\cdot\text{Cl}$ CT complex, similar to that previously reported by Herrmann in aqueous solutions of chloro and hypochloric acids.³⁷ The less intense second band at 290 nm is consequently assigned to a $\text{CH}_3\text{C}(\text{O})\text{CH}_2\cdot$ radical fragment, consistent with Hayon and co-workers.^{43,45}

DISCUSSIONS

Ultrafast Photochemistry. The electronic absorption spectra of the copper(II) complexes consist of highly intense UV bands corresponding to LMCT transitions, and near-IR bands of much

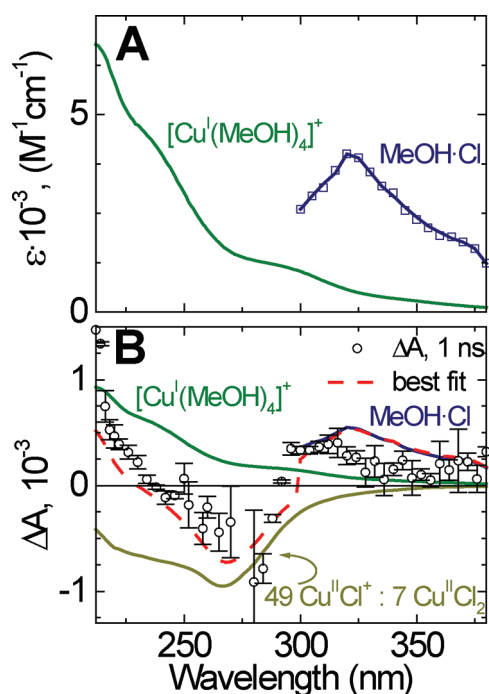


Figure 5. (A) Absorption spectra of Cl·MeOH CT complexes and $[\text{Cu}^{\text{I}}(\text{MeOH})_4]^+$ complexes in methanol obtained as described in the text. The extinction coefficient at the absorption maximum of the Cl·MeOH CT complex was assumed to be $4000 \text{ M}^{-1} \text{ cm}^{-1}$ equal to that reported for the Cl·H₂O CT complex.⁴² (B) The fit of the 1000-ps transient absorption spectrum of a 50 mM $\text{Cu}(\text{ClO}_4)_2/25 \text{ mM LiCl}$ methanol solution to the spectra of Cl·MeOH CT and $[\text{Cu}^{\text{I}}(\text{MeOH})_4]^+$ (assumed to be in equal concentrations), and the sum of the steady-state absorption spectra of $[\text{Cu}^{\text{II}}(\text{MeOH})_5\text{Cl}]^+$ and $[\text{Cu}^{\text{II}}(\text{MeOH})_4\text{Cl}_2]$. For the two latter complexes, the concentration ratio 49/7 is assumed as in Figure 2.

lower intensity assigned to symmetry forbidden ligand-field (LF) transitions between the d orbitals of a copper ion.^{24,32,33} The 255-nm excitation wavelength used in this work preferentially excites $[\text{Cu}^{\text{II}}(\text{MeOH})_5\text{Cl}]^+$, and the $[\text{Cu}^{\text{II}}(\text{MeOH})_6]^{2+}$ and $[\text{Cu}^{\text{II}}(\text{MeOH})_4\text{Cl}_2]$ complexes are also excited in a ratio of 1.0:0.33:0.16 based on the relative absorbance of these complexes in solution. The quantum yield of products for the least absorbing $[\text{Cu}^{\text{II}}(\text{MeOH})_6]^{2+}$ is five times less than for $[\text{Cu}^{\text{II}}(\text{MeOH})_5\text{Cl}]^+$ at 255 nm.^{23,24} The product quantum yields for $[\text{Cu}^{\text{II}}(\text{MeOH})_4\text{Cl}_2]$ and $[\text{Cu}^{\text{II}}(\text{MeOH})_5\text{Cl}]^+$ are comparable;²⁴ however, the relative absorption of the former is small (10% of the total absorbance at 255 nm). Furthermore, transient absorption experiments upon 255-nm excitation in acetonitrile solutions of copper(II), where only monochloro copper(II) complexes are excited, reveal a comparable width of the bleach signal (Supporting Information) as well as similar short-time dynamics. We, therefore, conclude that the photoexcitation of $[\text{Cu}^{\text{II}}(\text{MeOH})_5\text{Cl}]^+$ complexes dominates the dynamics observed in methanol solutions of copper(II).

Photochemical Cu–Cl bond breaking in $[\text{Cu}^{\text{II}}(\text{MeOH})_5\text{Cl}]^+$ may occur either via an ionic mechanism with the formation of a $[\text{Cu}^{\text{II}}(\text{MeOH})_5]^{2+}$ complex and a chloride anion, or via a radical mechanism with the formation of the $[\text{Cu}^{\text{I}}(\text{MeOH})_5]^+$ complex and a chlorine atom. As 255-nm excitation is into the LMCT transition of $[\text{Cu}^{\text{II}}(\text{MeOH})_5\text{Cl}]^+$, the latter cleavage mechanism is expected. Indeed, previous photochemical investigations

showed the formation of copper(I) complexes and formaldehyde consistent with a radical dissociation mechanism.²⁴ This is also in agreement with the detection of formaldehyde in solutions exposed to the 255-nm laser pulses in our work. It is well-known that Cl^\bullet atom fragments quickly form charge-transfer complexes with the surrounding solvent.^{36–43} CT complexes of chlorine atoms with “noncomplexing solvents” such as water, dichloromethane, and chloroform, exhibit broad absorption bands with maxima at around 310–335 nm.^{37,39–43} On the basis of the well-obeyed correlation between the absorption maximum of a CT complex involving a halogen atom acceptor and the ionization potential of a solvent donor, the band maximum of the MeOH·Cl CT complex is expected to lie at about 330 nm. This is in agreement with our observation of the absorption maximum of the MeOH·Cl CT complex at 320 nm, Figure 5A. As for the $[\text{Cu}^{\text{I}}(\text{MeOH})_5]^+$ fragment, its electronic absorption spectrum is not known. However, a coordination number of five is uncommon for Cu^{I} complexes.^{12,18} As a result, this fragment is expected to be unstable, giving rise to a relatively more stable $[\text{Cu}^{\text{I}}(\text{MeOH})_4]^+$ complex with intense absorption in the 210–230 nm range, Figure 5A.

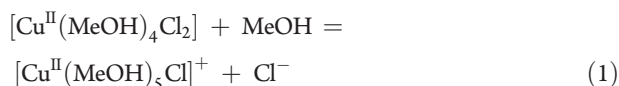
The spectral evolution of the short-time ΔA spectra (time delays, 0.2–10 ps) is much more complicated than one would expect for simple photodissociation of $[\text{Cu}^{\text{II}}(\text{MeOH})_5\text{Cl}]^+$. Narrowing and blue shifting of the broad, 310–384 nm transient absorption observed on a 0.3–10 ps time scale is inconsistent with a slight spectral shift characteristic of the formation and relaxation of Cl·solvent CT complexes,⁴⁰ bearing signatures of vibrational relaxation. Typically, vibrationally hot polyatomic molecules absorb to the red of the vibrationally relaxed species.⁴⁶ Therefore, the transient absorption emerging at the red wing of the steady-state spectrum of $[\text{Cu}^{\text{II}}(\text{MeOH})_5\text{Cl}]^+$ is assigned to vibrationally hot $[\text{Cu}^{\text{II}}(\text{MeOH})_5\text{Cl}]^+$. Spectral narrowing and blue-shifting of the transient absorption as a function of time manifests an increase in the Franck–Condon overlap with probe wavelengths within the steady-state spectrum, as hot $[\text{Cu}^{\text{II}}(\text{MeOH})_5\text{Cl}]^+$ undergoes vibrational relaxation. The observation of hot transient absorption of $[\text{Cu}^{\text{II}}(\text{MeOH})_5\text{Cl}]^+$ as early as 0.2 ps following excitation suggests that the parent complex excited into the LMCT state undergoes fast internal conversion, which populates highly excited vibrational states on the ground-state potential energy surface (Figure 4). The decay of electronically excited $[\text{Cu}^{\text{II}}(\text{MeOH})_5\text{Cl}]^+$ species is too fast to be resolved using the current time resolution of our instrument, but 0.2 ps provides an upper limit for the internal conversion process. Shorter probe wavelengths, cf. 312 and 234 nm, give a somewhat longer formation time, $\tau_1 = 0.4$ and 0.69 ps, respectively, since the slower vibrational relaxation process is mixed into the lifetime measured at these wavelengths as a result of spectral evolution of the hot parent complex. Subsequent vibrational relaxation on a several ps time scale (τ_2) leads to the repopulation of the vibrationally relaxed ground-state, and subsequently, the observed recovery of the $[\text{Cu}^{\text{II}}(\text{MeOH})_5\text{Cl}]^+$ ground-state bleach. We note that hydrogen bonding between the hot complex and solvent molecules provides a very efficient and fast energy dissipation pathway.^{47,48}

The long-time dynamics are consistent with the formation of MeOH·Cl CT complexes. Because of significant (120–160 kJ mol^{-1}) Cu–Cl radical bond dissociation energies reported for chloro Cu^{II} complexes,⁴⁹ we favor the formation of Cl^\bullet fragments from the excited state of $[\text{Cu}^{\text{II}}(\text{MeOH})_5\text{Cl}]^+$ as a result of photodissociation, rather than thermal decomposition

of the vibrationally hot ground-state species. The extinction coefficients of $[\text{Cu}^{\text{II}}(\text{MeOH})_5\text{Cl}]^+$ and $\text{MeOH}\cdot\text{Cl}$ are comparable (typical ϵ values for solvent $\cdot\text{Cl}$ CT complexes are $\sim 2000\text{--}4000\text{ M}^{-1}\text{ cm}^{-1}$ ^{42,43}), and both species should be noticeable in the ΔA spectra provided that they are formed in comparable yields. However, the spectral signature of vibrationally hot parent complexes dominates short-time dynamics. Therefore, we conclude that internal conversion is a major pathway for radiationless decay. LMCT excited states of transition metal ions such as $\text{Co}(\text{III})$, $\text{Fe}(\text{III})$, $\text{Cr}(\text{III})$, $\text{Cu}(\text{II})$, etc. are typically very short-lived.^{50–57} Internal conversion from LMCT excited states is interpreted to occur either directly to the ground state, or stepwise, via lower-lying LF excited states. In our work, the observed radical bond cleavage products are consistent with photodissociation taking place from the LMCT state. Notably, the observed short-time spectral evolution is consistent with absorption of vibrationally hot ground state species. The excited state absorption from the LF states of the $[\text{Cu}^{\text{II}}(\text{MeOH})_5\text{Cl}]^+$ species to the lowest LMCT state corresponds to wavelengths in the vicinity of 380 nm based on the energy gap between the maxima of the LMCT and LF bands (265 and 885 nm), i.e. it partially overlaps with the probed deep-near UV range. The fact that vibrational relaxation dominates the dynamics, does not allow us to safely rule out the involvement of these LF states in the overall photochemical path. Nevertheless, the present results strongly suggest that the electronically excited species in the LMCT state relax to the ground state via back electron transfer either directly or stepwise via extremely short-lived (<250 fs) LF excited states. Such short-lived LF states have been recently observed for a bioinorganic copper(II) complex, a blue copper protein (plastocyanin).⁵⁵

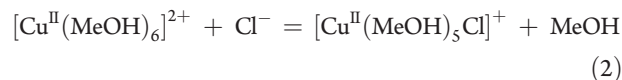
Photodissociation leads to the overcoordinated $[\text{Cu}^{\text{I}}(\text{MeOH})_5]^+$ fragments^{12,18} possessing vibrational energy excess. Therefore, these species are very likely to undergo further irreversible dissociation, giving rise to a tetraordinated copper(I) complex, $[\text{Cu}^{\text{I}}(\text{MeOH})_4]^+$. The 2.2-ps rise time of the transient absorption in the deep UV region (214 nm, Figure 4A) where the $[\text{Cu}^{\text{I}}(\text{MeOH})_4]^+$ species possess intense absorption is the likely spectroscopic manifestation of this decomposition.

The ground-state absorption bleach remains spectrally narrow to about 10 ps, indicative of the depletion of ground-state $[\text{Cu}^{\text{II}}(\text{MeOH})_5\text{Cl}]^+$ species. However, as a result of the photochemical decomposition of $[\text{Cu}^{\text{II}}(\text{MeOH})_5\text{Cl}]^+$, the ground-state equilibrium between the various copper(II) complexes becomes perturbed. Extremely large ligand exchange rates were reported for d^9 systems,¹³ and therefore, the spectral evolution of the ground-state bleach from other complexes present in the solution ($[\text{Cu}^{\text{II}}(\text{MeOH})_6]^{2+}$ and $[\text{Cu}^{\text{II}}(\text{MeOH})_4\text{Cl}_2]$) can be expected as a result of ground-state re-equilibration. Indeed, at longer delay times between 10 and 500 ps, the red shift and build-up of the negative ΔA signal between 258 and 293 nm, the region where the absorbance of $[\text{Cu}^{\text{II}}(\text{MeOH})_5\text{Cl}]^+$ decreases steeply, suggests a gradual depletion of the ground-state $[\text{Cu}^{\text{II}}(\text{MeOH})_4\text{Cl}_2]$ complexes via



The dichloro Cu^{II} complexes possess a molecular decadic extinction coefficient larger than the parent $[\text{Cu}^{\text{II}}(\text{MeOH})_5\text{Cl}]^+$ complexes between 260 and 380 nm. The development of the ground-state absorption bleach of $[\text{Cu}^{\text{II}}(\text{MeOH})_4\text{Cl}_2]$ ought to lead to the decay

of transient absorption in the red part of the spectrum, as observed. Similarly, the decay of transient absorption in the deep-UV range may be attributed to re-equilibration involving $[\text{Cu}^{\text{II}}(\text{MeOH})_6]^{2+}$ via



Note that our experiments suggest that the latter re-equilibration process occurs on a much longer time scale of several nanoseconds (~ 5.8 ns). On a time scale of several tens of picoseconds, the species involved in the photochemical reaction are already thermalized, and it is possible to use their steady-state spectra to assign the transient absorption ΔA spectra. The adequate fit of the 1000-ps ΔA spectrum includes a sum of the positive absorption contributions of the $\text{MeOH}\cdot\text{Cl}$ CT and $[\text{Cu}^{\text{I}}(\text{MeOH})_4]^+$ complexes (implying the occurrence of the photodissociation), and the negative contribution of the steady-state absorption spectra of two $[\text{Cu}^{\text{II}}(\text{MeOH})_5\text{Cl}]^+$ and $[\text{Cu}^{\text{II}}(\text{MeOH})_4\text{Cl}_2]$ complexes (their relative concentrations were assumed to be the same as those in Figure 2). In the fit, we used the assumption that the $[\text{Cu}^{\text{I}}(\text{MeOH})_5]^+$ intermediate completely and irreversibly dissociated to $[\text{Cu}^{\text{I}}(\text{MeOH})_4]^+$ at 1 ns after excitation, and we further postulated that the $\text{MeOH}\cdot\text{Cl}$ CT and $[\text{Cu}^{\text{I}}(\text{MeOH})_4]^+$ complexes exist in solution in equal amounts. Therefore, the concentration ratio of the $\text{MeOH}\cdot\text{Cl}$ CT and $[\text{Cu}^{\text{I}}(\text{MeOH})_4]^+$ complexes was constrained to 1:1 for the fit. The extinction coefficient at the absorption maximum of $\text{Cl}\cdot\text{MeOH}$ CT complexes was taken to be equal to that of $\text{Cl}\cdot\text{H}_2\text{O}$ CT complexes, $\epsilon = 4000\text{ M}^{-1}\text{ cm}^{-1}$.⁴² The $\epsilon = 4000\text{ M}^{-1}\text{ cm}^{-1}$ value represents an upper limit for $\text{Cl}\cdot\text{solvent}$ CT complexes because, e.g., $\epsilon = 2000\text{ M}^{-1}\text{ cm}^{-1}$ was reported for the $\text{Cl}\cdot\text{C}_6\text{H}_6$ CT complexes.⁴³ However, good fits were also obtained assuming smaller ϵ values for the $\text{Cl}\cdot\text{MeOH}$ CT complexes in the $2000\text{--}4000\text{ M}^{-1}\text{ cm}^{-1}$ range; see the Supporting Information. Thus, the conclusion that the equilibration between $[\text{Cu}^{\text{II}}(\text{MeOH})_5\text{Cl}]^+$ and $[\text{Cu}^{\text{II}}(\text{MeOH})_4\text{Cl}_2]$ is complete at 1 ns is not too sensitive to the choice of the ϵ value for the $\text{Cl}\cdot\text{MeOH}$ CT complexes. The fit of the 1000-ps ΔA spectrum using the negative contribution of the entire steady-state absorption spectrum (implying complete re-equilibration of all three complexes) deviates from the experimental data points in the deep-UV part of the spectrum, suggesting incomplete re-equilibration of the $[\text{Cu}^{\text{II}}(\text{MeOH})_6]^{2+}$ species; see the Supporting Information.

Ion and Neutral Diffusion. The ligand exchange reaction (eq 1) involves two neutral species: methanol in vast excess and $[\text{Cu}^{\text{II}}(\text{MeOH})_4\text{Cl}_2]$. Under the assumption that a methanol molecule approaches the first coordination sphere by diffusion, and that this diffusive approach is a limiting step in eq 1, the corresponding rate constant (k_D , $\text{M}^{-1}\text{ s}^{-1}$) can be described by the Smoluchowski relationship⁵⁸

$$k_D = 4\pi \cdot 10^{-3} N_A D (R_1 + R_2) \quad (3)$$

where $D = D_1 + D_2$ is the total diffusion coefficient equal to the sum of the individual diffusion coefficients of the involved reagents, R_1 and R_2 are the radii of the reagent species assumed spherical, and N_A is Avogadro's number ($6.02 \times 10^{23}\text{ mol}^{-1}$). Here, 1 and 2 correspond to $[\text{Cu}^{\text{II}}(\text{MeOH})_4\text{Cl}_2]$ and CH_3OH , respectively. The size of the $[\text{Cu}^{\text{II}}(\text{MeOH})_4\text{Cl}_2]$ complex is much larger than that of the CH_3OH molecule, and therefore, $D \approx D_2$, where $D_2 = 1.78 \times 10^{-5}\text{ cm}^2\text{ s}^{-1}$ ⁵⁹ is the coefficient of methanol self-diffusion at 293 K. The effective radius of $[\text{Cu}^{\text{II}}(\text{MeOH})_4\text{Cl}_2]$ can be estimated as an average sum of the metal–ligand bond distance and ligand effective radius for which the following values are assumed: $2.2 \times 10^{-8}\text{ cm}$ ($\text{Cu}\text{--}\text{O}$ bond distance)

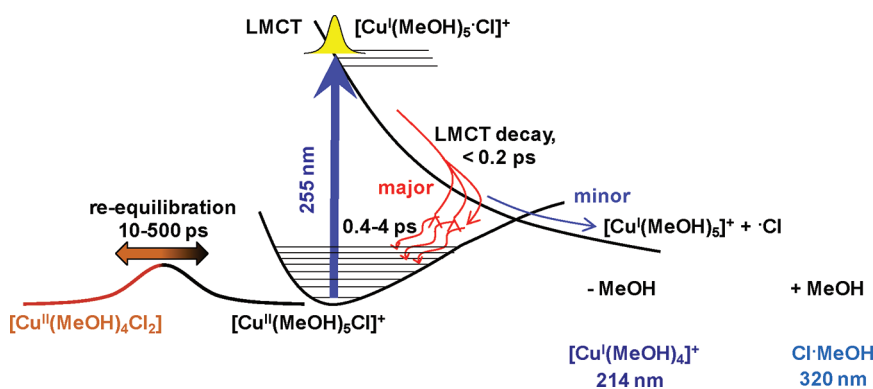


Figure 6. Suggested mechanism of the photodissociation of a $[\text{Cu}^{\text{II}}(\text{MeOH})_5\text{Cl}]^+$ complex upon 255-nm excitation into its LMCT state.

and 2.5×10^{-8} cm (Cu–Cl distance) based on the known structure of aqueous Cu^{II} complex,¹⁵ 1.81×10^{-8} cm (Cl^- ionic radius⁶⁰) and 1.9×10^{-8} cm (CH_3OH effective radius⁶¹). This yields $R_1 = 4.2 \times 10^{-8}$ cm. For methanol, the effective radius is $R_2 = 1.9 \times 10^{-8}$ cm.⁶¹ The k_{D} value thus obtained is equal to $8.1 \times 10^9 \text{ M}^{-1} \text{ s}^{-1}$. In the nearly neat methanol solutions (assumed concentration, 24.7 M), $k_{\text{D}} = 8.1 \times 10^9 \text{ M}^{-1} \text{ s}^{-1}$ yields an inverse diffusion-limited rate of 5 ps.

To predict diffusion-controlled rates for reactions between ions, e.g., eq 2, Debye's theory based on bimolecular encounters can be used. At low electrolyte concentrations, Debye's diffusion-controlled rate constant k_{D} is expressed

$$k_{\text{D}} = 4\pi 10^{-3} N_{\text{A}} D r \left(\frac{U_{\text{e}}/k_{\text{B}}T}{e^{U_{\text{e}}/k_{\text{B}}T} - 1} \right) \quad (4)$$

where $D = D_1 + D_2$ is the total diffusion coefficient of two ions 1 (Cl^-) and 2 ($[\text{Cu}(\text{MeOH})_6]^{2+}$) with charges z_1 and z_2 , N_{A} is the Avogadro's number, k_{B} is the Boltzmann constant, T is the absolute temperature, r is the closest distance between two interacting ions, and U_{e} is the electrostatic potential. In its turn, $U_{\text{e}} = z_1 z_2 e^2 / 4\pi\epsilon r$, where ϵ is the solvent dielectric constant. The average Cu–Cl bond distance in aqueous $[\text{Cu}(\text{H}_2\text{O})_5\text{Cl}]^+$ complexes is about 2.5×10^{-8} cm,¹⁵ and this value was adopted for r . Because the size of Cl^- is much smaller than that of $[\text{Cu}(\text{MeOH})_6]^{2+}$, the D value can be considered is mainly due to a chloride ion. The latter D_1 value can be estimated to be equal to $2.15 \times 10^{-5} \text{ cm}^2 \text{ s}^{-1}$ at $T = 293 \text{ K}$ using the Stokes–Einstein equation, $D_1 = k_{\text{B}}T / 6\pi\eta a$, where η is solvent viscosity (0.55 cP^{62}), and a is the ionic radius of Cl^- (1.81×10^{-8} cm). The U_{e} value is calculated to be 4.44×10^{-14} erg using $z_1 = 1$, $z_2 = 2$ for the reacting species and $\epsilon = 33$ ⁶² for methanol. The diffusion-limited rate constant is estimated to be $k_{\text{D}} = 2.23 \times 10^9 \text{ M}^{-1} \text{ s}^{-1}$. The inverse rate of the process is 18 ns for the $[\text{Cl}^-] = 25 \text{ mM}$ used, which is comparable to the 10-ns time scale estimated from the experiment.

Exchange Mechanism. The Jahn–Teller distortion of Cu^{II} complexes renders the bond between Cu and axial ligand labile. The distortion axis jumps very rapidly,¹⁶ therefore, when chloride ligands appear in the axial positions, a Cu–Cl bond in $[\text{Cu}^{\text{II}}(\text{MeOH})_4\text{Cl}_2]$ likely dissociates (Figure 6). The calculated inverse diffusion-controlled rate for chloride ligand substitution by a methanol molecule via eq 1 (5 ps) is significantly smaller than the experimental lifetime (150–250 ps). Therefore, the reaction is controlled by an energy barrier, and can be thought to occur via a dissociative mechanism.^{63,64} The solvent exchange reaction for a coordinated methanol molecule with the bulk solution in the

related $[\text{Cu}^{\text{II}}(\text{MeOH})_6]^{2+}$ complexes was similarly reported to occur via an interchange dissociative mechanism.¹⁶ Thus, reaction (eq1) occurs in a stepwise manner along the reaction coordinate. Methanol from the second coordination sphere substitutes the vacancy of the copper metal center when the chloride ligand departs the complex. The energy barrier comes both from bond dissociation enthalpy and entropy contributions, where the latter probably arises from the rearrangement of the solvent molecules around the charged complex. Indeed, the departing Cl^- ligand and the approaching CH_3OH ligand have to disrupt the H-bonding solvent network, which is further ordered by the polarization forces exerted by a Cu^{2+} ion.

The exchange reaction described by eq 2 is diffusion-limited. It can be thought to occur via the preassociation mechanism described by Eigen and Wilkins.¹³ In this mechanism, the Cl^- ion diffuses into the second coordination sphere and forms an ion pair with the $[\text{Cu}^{\text{II}}(\text{MeOH})_6]^{2+}$ complex by electrostatic interactions. When successful collisions are made, the Cl^- ion replaces one of the coordinated CH_3OH ligands.

CONCLUSIONS

Ultrafast transient absorption spectroscopy with deep-near UV probing (212–384 nm) was used to investigate the radiationless relaxation pathways of a model monochloro complex of copper(II) in methanol solutions promoted into its ligand-to-metal charge-transfer excited state upon 255-nm excitation. The chemical composition of the parent methanol solutions containing copper(II) (50 mM $\text{Cu}(\text{ClO}_4)_2$ /25 mM LiCl) ensured preferential photoexcitation of $[\text{Cu}^{\text{II}}(\text{MeOH})_5\text{Cl}]^+$ in the presence of other two copper(II) complexes, $[\text{Cu}^{\text{II}}(\text{MeOH})_6]^{2+}$ and $[\text{Cu}^{\text{II}}(\text{MeOH})_4\text{Cl}_2]$. The dynamics of the short-lived nonthermalized states and reaction intermediates are traced through the time-dependent spectral evolution. The electronically excited $[\text{Cu}^{\text{II}}(\text{MeOH})_5\text{Cl}]^+$ species undergo internal conversion via back electron transfer to the vibrationally hot electronic ground state of $[\text{Cu}^{\text{II}}(\text{MeOH})_5\text{Cl}]^+$ (major path) (Figure 6) and Cu–Cl radical bond dissociation (minor path). An upper limit for the time scale of the radiationless decay of the LMCT state is ~ 0.2 ps. The subsequent short-time spectral evolution of the transient absorption ΔA spectra manifest vibrational relaxation of hot $[\text{Cu}^{\text{II}}(\text{MeOH})_5\text{Cl}]^+$ occurring with a distribution of time constants between 0.4 and 4 ps, as well as a rise (time constant, 2.2 ps) in the deep-UV absorbing tetra-coordinated Cu^{I} ($[\text{Cu}^{\text{I}}(\text{MeOH})_4]^+$) complex formed as a result of the nascent overcoordinated Cu^{I} fragment ($[\text{Cu}^{\text{I}}(\text{MeOH})_5]^+$) losing a MeOH ligand. Some

absorption of the MeOH·Cl charge-transfer complexes is present to the longest time delays investigated (1050 ps), indicating small but irreversible photodecomposition of the parent complexes. Small photodecomposition yield of the complexes observed can be explained by competing ultrafast internal conversion from the electronically excited LMCT state. The photochemical decomposition of $[\text{Cu}^{\text{II}}(\text{MeOH})_5\text{Cl}]^+$ perturbs the equilibrium between the copper(II) complexes present in the solution. The evolution of the long-time ΔA signals is consistent with the fast (time scale, 10–500 ps) for the depletion of the ground-state $[\text{Cu}^{\text{II}}(\text{MeOH})_4\text{Cl}_2]$ complexes and much slower (time scale, several nanoseconds) depletion of the ground-state $[\text{Cu}^{\text{II}}(\text{MeOH})_6]^+$. The comparison of the experimentally observed re-equilibration rate constants and diffusion-controlled rate constants calculated for ion and neutral species exchange suggests the dissociative and preassociative mechanisms for the Cl^- -to-MeOH substitution in $[\text{Cu}^{\text{II}}(\text{MeOH})_4\text{Cl}_2]$ and the MeOH-to- Cl^- substitution in $[\text{Cu}^{\text{II}}(\text{MeOH})_6]^{2+}$, respectively.

■ ASSOCIATED CONTENT

S Supporting Information. (i) Energy dependence of the transient absorption signals for a 50 mM $\text{Cu}(\text{ClO}_4)_2/25$ mM LiCl methanol solution at 255/312 nm pump/probe wavelengths, (ii) 0.5-ps transient absorption ΔA spectra measured in methanol and acetonitrile solutions, and (iii) a comparison of the fitted 1000-ps transient absorption spectrum using different values for the molecular decadic extinction coefficient of Cl^- ·MeOH CT complexes and different degrees of ground-state re-equilibration. This material is available free of charge via the Internet at <http://pubs.acs.org>.

■ AUTHOR INFORMATION

Corresponding Author

*E-mail: atarnov@bgsu.edu.

Present Addresses

[†]School of Basic Sciences, Indian Institute of Technology (IIT), Mandi, Himachal Pradesh, 175 001 India.

[‡]Department of Chemistry, University of California, Irvine, California, 92697-2025 United States.

■ ACKNOWLEDGMENT

This work was supported by the NSF CAREER award (Grant CHE-0847707, A.N.T.). Discussions with Prof. M. Yu. Skripkin (St. Petersburg State University) are gratefully acknowledged.

■ REFERENCES

- (1) Prohaska, J. R. *Physiol. Rev.* **1987**, *67*, 858–901.
- (2) Shorrocks, V. Copper and Human Health – A Review. Technical Note 34. [Online] **1984**, Copper Development Association. <http://www.copperinfo.co.uk/health/> (accessed January, 18, 2011).
- (3) Harris, E. D. Copper in Human and Animal Health. In *Trace Elements in Health*; Rose, J., Ed.; Butterworths: London, 1983; p 44.
- (4) Sorenson, J. R. *J. Prog. Med. Chem.* **1978**, *15*, 211–260.
- (5) Barbean, A. *Int. J. Neurol.* **1976**, *11*, 17–27.
- (6) Underwood, E. J. Copper. In *Trace Elements in Humans and Animals*, 4th ed.; Academic Press: New York, 1971.
- (7) Danks, D. M.; Campbell, P. E.; Stevens, B. J.; Mayne, V.; Cartwright, E. *Pediatrics* **1972**, *50*, 188–201.
- (8) Danks, D. M.; Stevens, B. J.; Campbell, P. E.; Gillespie, J. M.; Walker-Smith, J.; Bloomfield, J.; Turner, B. *Lancet* **1972**, *1*, 1100–1102.

- (9) Owen, C. A. Jr. Copper Deficiency and Toxicity, Acquired and Inherited. In *Plants, Animals and Men*; Noyes Publications: Norwich, NY, 1981.
- (10) Sternlieb, I. *Med. Radiogr. Photogr.* **1966**, *42*, 14–15.
- (11) Walshe, J. M. *Lancet* **1960**, *i*, 188–192.
- (12) Cotton, F. A.; Wilkinson, G. *Advanced Inorganic Chemistry: A Comprehensive Text*, 4th ed.; Wiley Interscience Publishers: New York, 1980.
- (13) Eigen, M.; Wilkins, R. G. *Adv. Chem. Ser.* **1965**, *49*, 55–80.
- (14) Chaboy, J.; Munoz-Paez, A.; Merklung, P. J.; Marcos, E. S. *J. Chem. Phys.* **2006**, *124*, 064509.
- (15) Smirnov, P. R.; Trostin, V. N. *Russ. J. Gen. Chem.* **2009**, *79*, 1591–1599.
- (16) Helm, L.; Merbach, A. E. *Chem. Rev.* **2005**, *105*, 1923–1959.
- (17) Helm, L.; Lincoln, S. F.; Merbach, A. E.; Zbindenla, D. *Inorg. Chem.* **1986**, *25*, 2550–2552.
- (18) Persson, I.; Pennerhahn, J. E.; Hodgson, K. O. *Inorg. Chem.* **1993**, *32*, 2497–2501.
- (19) de Almeida, K. J.; Rinkevicius, Z.; Hugosson, H. W.; Ferreira, A. C.; Agren, H. *Chem. Phys.* **2007**, *332*, 176–187.
- (20) de Almeida, K. J.; Murugan, N. A.; Rinkevicius, Z.; Hugosson, H. W.; Vahtras, O.; Agren, H.; Cesar, A. *Phys. Chem. Chem. Phys.* **2009**, *11*, 508–519.
- (21) Pasquarello, A.; Petri, I.; Salmon, P. S.; Parisel, O.; Car, R.; Toth, E.; Powell, D. H.; Fischer, H. E.; Helm, L.; Merbach, A. E. *Science* **2001**, *291*, 856–859.
- (22) Kochi, J. K. *J. Am. Chem. Soc.* **1962**, *84*, 2121–2127.
- (23) da Silva, P. A. C.; David, P. G. *Bull. Chem. Soc. Jpn.* **1982**, *55*, 2673–2674.
- (24) David, P. G.; da Silva, P. A. C. *Bull. Chem. Soc. Jpn.* **1985**, *58*, 3566–3569.
- (25) Kaczmarek, H.; Kaminska, A.; Linden, L. A.; Rabek, J. F. *Polymer* **1996**, *37*, 4061–4068.
- (26) Glebov, E. M.; Plyusnin, V. F.; Grivin, V. P.; Krupoder, S. A.; Liskovskaya, T. I.; Danilovich, V. S. *J. Photochem. Photobiol. A: Chem.* **2000**, *133*, 177–183.
- (27) Pal, S. K.; Mereshchenko, A. S.; El-Khoury, P. Z.; Tarnovsky, A. N. *Chem. Phys. Lett.* **2011**, *507*, 69–73.
- (28) Voskresenska, V.; Wilson, R. M.; Panov, M.; Tarnovsky, A. N.; Krause, J. A.; Vyas, S.; Winter, A. H.; Hadad, C. M. *J. Am. Chem. Soc.* **2009**, *131*, 11535–11547.
- (29) Reuther, A.; Laubereau, A.; Nikogosyan, D. N. *Opt. Commun.* **1997**, *141*, 180–184.
- (30) Rasmusson, M.; Tarnovsky, A. N.; Åkesson, E.; Sundström, V. *Chem. Phys. Lett.* **2001**, *335*, 201–208.
- (31) Hathaway, B. J.; Holah, D. G.; Postlethwaite, J. D. *J. Chem. Soc.* **1961**, 3215–3218.
- (32) Khan, M. A.; Meullemeestre, J.; Schwing, M. J.; Vierling, F. *Inorg. Chem.* **1989**, *28*, 3306–3309.
- (33) Khan, M.; Bouet, G.; Vierling, F.; Meullemeestre, J.; Schwing, M. J. *Transit. Met. Chem.* **1996**, *21*, 231–234.
- (34) KTH - Chemistry/Chemical Equilibrium Diagrams; <http://www.kemi.kth.se/medusa/> (accessed January, 18, 2011).
- (35) Nash, T. *Biochem. J.* **1953**, *55*, 416–421.
- (36) Strachan, A. N.; Blacet, F. E. *J. Am. Chem. Soc.* **1955**, *77*, 5254–5257.
- (37) Herrmann, H. *Phys. Chem. Chem. Phys.* **2007**, *9*, 3935–3964.
- (38) Kitchen, D. C.; Myers, T. L.; Butler, L. J. *J. Phys. Chem.* **1996**, *100*, 5200–5204.
- (39) Thomsen, C. L.; Madsen, D.; Poulsen, J. A.; Thøgersen, J.; Knak Jensen, S. J.; Keiding, S. R. *J. Chem. Phys.* **2001**, *115*, 9361–9369.
- (40) Elles, C. G.; Cox, M. J.; Barnes, L. G.; Crim, F. F. *J. Phys. Chem. A* **2004**, *108*, 10973–10979.
- (41) Chateaneuf, J. E. *J. Org. Chem.* **1999**, *64*, 1054–1055.
- (42) Klänning, U. K.; Wolff, T. *Ber. Bunsen-Ges. Phys. Chem.* **1985**, *89*, 243–245.
- (43) Treinin, A.; Hayon, E. *J. Am. Chem. Soc.* **1975**, *97*, 1716–1721.

- (44) Pal, S. K.; Mereshchenko, A. S.; El-Khoury, P. Z.; Tarnovsky, A. N. *Chem. Phys. Lett.* **2011**, *507*, 69–73.
- (45) Nakashima, N.; Hayon, E. *J. Phys. Chem.* **1971**, *75*, 1910–1914.
- (46) Owrutsky, J. C.; Rafferty, D.; Hochstrasser, R. M. *Annu. Rev. Phys. Chem.* **1994**, *45*, 519–555.
- (47) Kovalenko, S. A.; Schanz, R.; Hennig, H.; Ernsting, N. P. *J. Chem. Phys.* **2001**, *115*, 3256–3273.
- (48) Middleton, C. T.; Boiko Cohen, B.; Kohler, B. *J. Phys. Chem. A* **2007**, *111*, 10460–10467.
- (49) Revesz, A.; Milko, P.; Zabka, J.; Schroeder, D.; Roithova, J. *J. Mass Spectrom.* **2010**, *45*, 1246–1252.
- (50) McCusker, J. K.; Walda, K. N.; Magde, D.; Hendrickson, D. N. *Inorg. Chem.* **1993**, *32*, 394–399.
- (51) Pozdnyakov, I. P.; Plyusnin, V. F.; Tkachenko, N.; Lemmetyinen, H. *Chem. Phys. Lett.* **2007**, *445*, 203–207.
- (52) Plyusnin, V. F.; Kolomeets, A. V.; Grivin, V. P.; Larionov, S. V.; Lemmetyinen, H. *J. Phys. Chem. A* **2011**, *115*, 1763–1773.
- (53) Juban, E. A.; McCusker, J. K. *J. Am. Chem. Soc.* **2005**, *127*, 6857–6865.
- (54) Edington, M. D.; Diffey, W. M.; Doria, W. J.; Riter, R. E.; Beck, W. F. *Chem. Phys. Lett.* **1997**, *275*, 119–126.
- (55) Nagasawa, Y.; Fujita, K.; Katayama, T.; Ishibashi, Y.; Miyasaka, H.; Takabe, T.; Nagao, S.; Hirota, S. *Phys. Chem. Chem. Phys.* **2010**, *12*, 6067–6075.
- (56) Ando, K. *J. Phys. Chem. B* **2008**, *112*, 250–256.
- (57) Delfino, I.; Manzoni, C.; Sato, K.; Dennison, C.; Cerullo, G.; Cannistraro, S. *J. Phys. Chem. B* **2006**, *110*, 17252–17259.
- (58) Rice, S. A. In *Diffusion-Limited Reactions*; Bamford, C. H., Tipper, C. F. H., Compton, R. G., Eds.; Comprehensive Chemical Kinetics 25; Elsevier: Amsterdam, The Netherlands, 1985; pp 3–46.
- (59) Hurlle, R. L.; Easteal, A. J.; Woolf, L. A. *J. Chem. Soc. Faraday Trans. I* **1985**, *81*, 769–779.
- (60) Shannon, R. D. *Acta Crystallogr., Sect. A* **1976**, *32*, 751–767.
- (61) Ben-Amotz, D.; Herschbach, D. R. *J. Phys. Chem.* **1990**, *94*, 1038–1047.
- (62) *CRC Handbook of Chemistry and Physics*, 90th ed.; Lide, D. R., Ed.; CRC Press: Boca Raton, FL, 2009.
- (63) Richens, D. T. *Chem. Rev.* **2005**, *105*, 1961–2002.
- (64) Ma, H.; Wan, C.; Zewail, A. H. *Proc. Acad. Natl. Sci. U.S.A.* **2008**, *105*, 12754–12757.